Enhancement of thermal conductivity across the metal-insulator transition in vanadium dioxide

Lu Chen, Ziji Xiang, Colin Tinsman, Tomoya Asaba, Qing Huang, Haidong Zhou, and Lu Li

Citation: Appl. Phys. Lett. **113**, 061902 (2018); doi: 10.1063/1.5042089
View online: https://doi.org/10.1063/1.5042089
View Table of Contents: http://aip.scitation.org/toc/apl/113/6
Published by the American Institute of Physics

Enhancement of thermal conductivity across the metal-insulator transition in vanadium dioxide

Lu Chen,[1,a)] Ziji Xiang,[1] Colin Tinsman,[1] Tomoya Asaba,[1] Qing Huang,[2] Haidong Zhou,[2] and Lu Li[1,b)]
[1]*Department of Physics, University of Michigan, Ann Arbor, Michigan 48109, USA*
[2]*Department of Physics and Astronomy, The University of Tennessee, Knoxville, Tennessee 37996, USA*

(Received 29 May 2018; accepted 20 July 2018; published online 9 August 2018)

Metal-to-insulator transition (MIT) in vanadium dioxide (VO_2) was investigated by electrical and thermal transport measurements. We report an order-of-magnitude enhancement of thermal conductivity across the MIT region in the VO_2 single crystal. The magnetic field dependent measurement reveals that the thermal conductivity peak does not show an obvious dependence on the magnetic field, which indicates that the enhancement of thermal conductivity could come from neutral heat carriers such as phonons. Our experiment provides a direction of achieving thermal management in phase-change materials. *Published by AIP Publishing.*
https://doi.org/10.1063/1.5042089

As a strongly correlated system, VO_2 undergoes a first order metal-to-insulator phase transition at around $T_s = 340$ K due to a crystal structure and electronic structure change.[1] The low-temperature insulating phase has a monoclinic structure (M, $P2_1/c$) with a bandgap $E_g \approx 0.6$ eV, while the high-temperature metallic phase is characterized by a rutile crystalline structure (R, $P4_2/mnm$).[2] The metal-to-insulator transition (MIT) is accompanied by a significant change in the electrical conductivity and the thermopower.[1,3] The transition temperature can be tuned over a wide range by aliovalent ion doping,[4] external strain,[5] and external electrical field.[6] As a typical example of phase-change material, VO_2 provides a potential platform for achieving electronic and optical devices.[7,8]

The nature of the MIT is still unclear due to the complex interplay among several degrees of freedom (charge, lattice, orbital, and spin). At a temperature around the MIT, the metallic tetragonal and insulating rutile phases coexist in this material and induce complicated domain structures, which significantly affect the transition characteristics, such as the broadening of the MIT.[9] A photoinduced metal-like phase of monoclinic VO_2 was reported by combining ultrafast electron diffraction and infrared transmissivity experiments, which indicates that there exists a metastable state within the transition that retains the lattice distortion of the insulating phase but acquires metal-like mid-infrared optical properties.[10] Recently, a thermal conductivity measurement has revealed a violation of the Wiedemann-Franz law by observing an order-of-magnitude decrease in the Lorentz number at the high-temperature metallic phase in the vicinity of the MIT.[3] This unusually low electronic thermal conductivity and the breakdown of the Wiedemann-Franz law indicate that the charge and heat carriers diffuse differently in this strongly correlated electron fluid.

In order to further understand the nature of the MIT, we conduct the electrical and thermal transport measurements in VO_2 single crystals. A significant decrease in the Seebeck coefficient accompanied by a 10^4–10^5 orders of magnitude increase in the electrical conductivity was observed across the transition. However, the thermal conductivity is enhanced by 1 order of magnitude at the transition temperature T_s. This thermal conductivity peak does not show apparent dependence on the magnetic field up to 13.9 T, which indicates that the heat carriers are neutral and do not interact with the external magnetic field. The strong enhancement of thermal conductivity likely results from the softening of certain phonon modes at the phase transition.[11,12]

The single crystal VO_2 samples being used in our experiments are grown by the chemical vapor transport method.[13,14] Typical single crystals are needle-like with the crystal c axis along the axial direction, which have lengths between 1 and 2 mm [shown in Fig. 1(a)]. The electrical and thermal transport measurements are conducted in our home-developed high-temperature vacuum probe. The temperature of the probe is controlled using a Lakeshore model 336 cryogenic temperature controller. The magnetic field dependent thermal measurement is conducted in a Physical

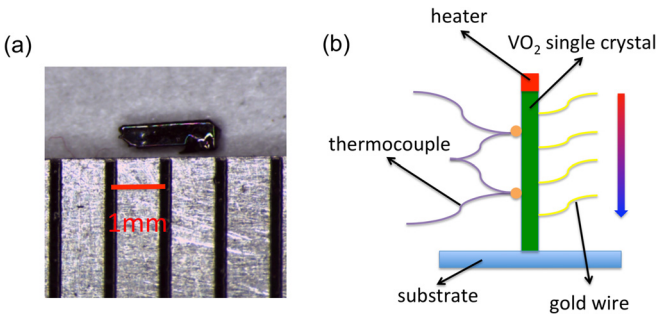

FIG. 1. (a) Typical VO_2 single crystals besides a mm scale. (b) Schematics of the experimental setup. A bar-shaped VO_2 single crystal stands vertically on a sapphire substrate with a resistive heater mounted on top of the sample. Four gold wires are used to conduct the four-lead resistance measurement as well as the thermopower measurement. Two shorted thermocouples are used to measure the temperature gradient along the sample. The arrow on the right-hand side indicates the direction of the heat flow.

a)Electronic mail: chelu@umich.edu
b)Electronic mail: luli@umich.edu

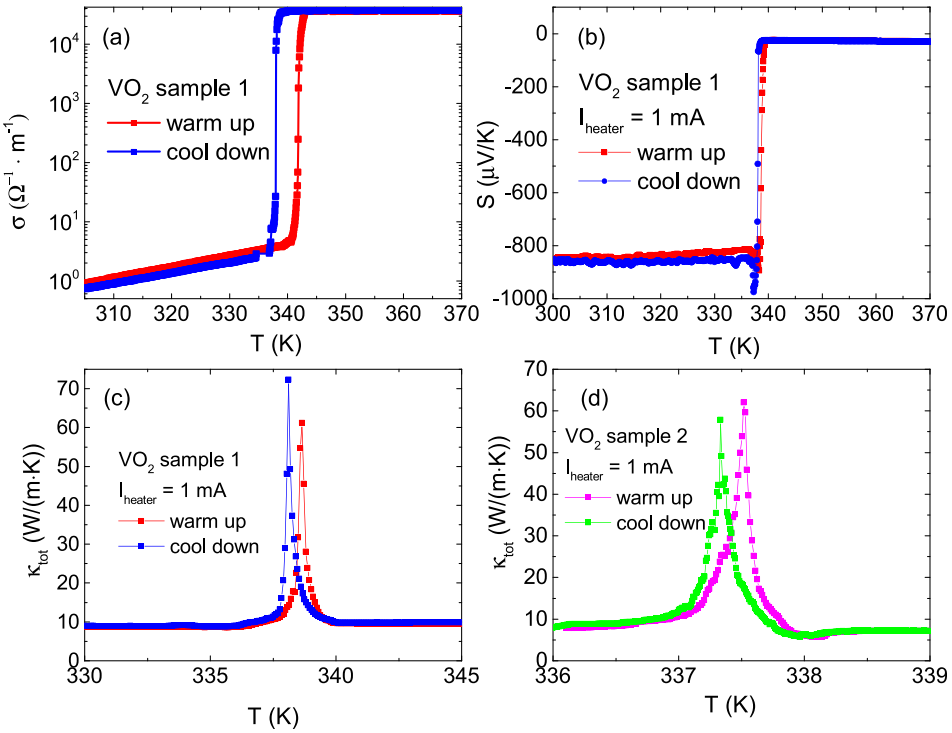

FIG. 2. (a) Four-probe electrical conductivity σ vs. T in VO_2 sample 1. (b) Seebeck coefficient S vs. T for VO_2 sample 1. The sample temperature was swept at a rate of 0.1 K/min. The difference of the transition temperature T_s between (a) and (b) results from the heating across the sample in the Seebeck measurement. (c) Measured total thermal conductivity κ_{tot} vs T for VO_2 sample 1 at the same T sweeping rate as Panel (b). The thermal conductivity peaks with an about 8–9 times increase across the metal-insulator transition. (d) Measured total thermal conductivity κ_{tot} vs. T for VO_2 sample 2 with a slower sweeping speed of temperature (~0.01 K/min). The enhancement of thermal conductivity signal is reproduced in sample 2. In (a) and (d), red (magenta) curves denote warming up, while blue (green) curves denote cooling down.

Properties Measurement System (PPMS) DynaCool from Quantum Design.

Figure 1(b) shows the schematic of our experimental setup. A needle-shaped VO_2 single crystal is mounted vertically on a sapphire substrate. A resistive heater is mounted on top of the sample, which can provide a thermal gradient along the c axis of the sample. Four electrical contacts are placed consecutively on the front side of the sample with H20E silver epoxy from Epo-tek, which can be used to conduct the four-lead resistance measurement as well as the thermal power measurement. Two type E thermocouples are mounted on the back side of the sample to measure the temperature gradient across the sample. In order to prevent the thermocouple from electrically shorted to the sample, the thermocouple junction is thermally linked to the sample by a small amount of thermal joint compound. Two ends of the thermocouples with the same material are shorted together. The voltage across the two un-shorted ends indicates the temperature difference between these two thermocouple junctions. The whole setup is glued on the heat sink of the high-temperature probe by H grease.

The four-lead resistance is measured by applying a low-frequency AC current through the sample with a Keithley 6221 DC and AC current source. The voltage across the sample is measured using a Stanford Research 830 DSP lock-in amplifier. The thermal power and thermal conductivity are measured by a pulsed power technique.[15] A periodic ac current ($f = 0.01$ Hz) is applied to the heater which seated on top of the sample by the current source. A small temperature gradient is generated between the heater and the heat sink. The temperature of the sample is adjusted by a global heater on the probe, which varies with a speed of 0.1 K/min in the experiment. The thermal power is measured through two of the electrical contacts using a Keithley 2182A nanovoltmeter. The voltage across the two thermocouples is measured using another Keithley 2182A nanovoltmeter. In our measurement, we carried out a dense temperature-dependent measurement only across the MIT region to reduce the material cracking due to the thermal cycles.

Figure 2(a) shows the temperature dependent electrical conductivity measured from 300 K to 370 K. The sample undergoes a metal to insulator transition around 340 K with the conductivity increasing about a factor of 10^4–10^5 and a thermal hysteresis loop appearing at T_s between warming up and cooling down, similar to previous results in VO_2 single crystals and thin films.[1,5,16] The difference between the transition temperature during warm up and cool down is around 4 K. The Seebeck coefficient is large and electron-like (shown as the negative sign) in the low temperature insulating state. The magnitude of S vs. temperature T is shown in Fig. 2(b). The Seebeck coefficient S starts to decrease from 850 μV/K for the insulating state to 26 μV/K for the metallic state at around $T_s = 338$ K. The constant value of S in the metallic state is consistent with the previous experimental results in bulk VO_2 single crystals,[1] microbeams,[17] and thin films.[18,19]

In bulk VO_2, it was reported that the total thermal conductivity κ_{tot} almost remains constant[1,3] or decreases[20] very slightly with temperature increases across the MIT. The temperature dependent thermal conductivity measured in VO_2 sample 1 is shown in Fig. 2(c). The thermal conductivity in the semiconductor states and the metallic states only differs by ~0.9 W/(m · K), which is about 4.5 times larger than the previously measured value in the VO_2 nanobeam [~0.2 W/(m · K)].[3] This difference is mainly because Ref. 3 used single-crystal VO_2 nanobeams while we used the VO_2 bulk single crystal. A larger thermal conductivity suggests a longer mean free path and less disorder in our bulk single crystal samples. We focused on the thermal conductivity in detail across the MIT and found that the thermal conductivity peaks with an increase of about 8–9 times within the MIT. This anomalous peak in thermal conductivity only exists

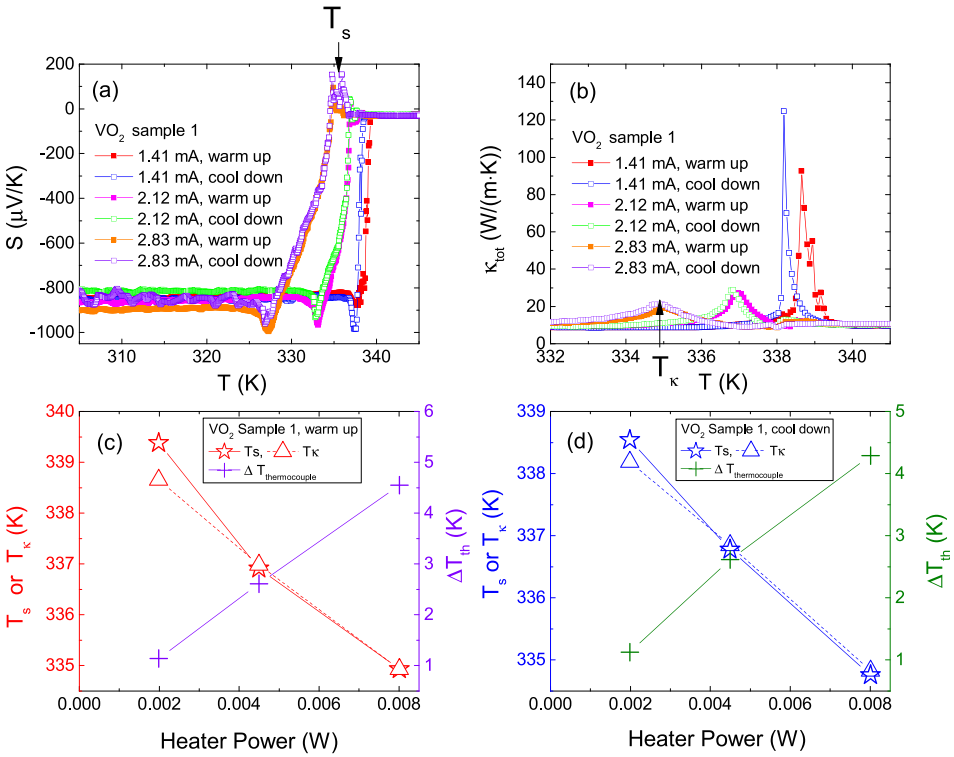

FIG. 3. (a) Temperature-dependent Seebeck coefficient S measured in VO_2 sample 1 with different heater currents. The AC current going through the heater I_{heater} ranges from 1.41 mA to 2.83 mA (peak value). The transition temperature T_s for thermal power is defined as the temperature when the entire sample enters the metallic state. T_s shifts towards lower temperature with higher heater power. (b) Total thermal conductivity κ_{tot} vs. T in VO_2 sample 1 with different heater currents. The peak position of thermal conductivity T_κ also decreases with the heater power. (c) Left axis: T_s and T_κ vs. heater power during warm up. Right axis: the temperature difference between the two thermocouples ΔT_{th} vs. heater power during warm up. (d) Left axis: T_s and T_κ vs. heater power during cool down. Right axis: the temperature difference between the two thermocouples ΔT_{th} vs. heater power during cool down. Solid and dashed lines are guides to the eyes.

within a very narrow temperature range inside the transition region (~2 K with $I_{heater} = 1.41$ mA), and it requires a very slow sweeping rate of global T to reveal such a narrow peak. Figure 2(c) is taken with a temperature sweeping speed of 0.1 K/min. This anomalous peak is repeated in VO_2 sample 2 with a slower sweeping speed (~0.01 K/min) [shown in Fig. 2(d)]. This sharp peak was likely missed in Ref. 3 because they only used a steady-state method which did not track dense enough data points within the MIT.

To study the self-heating effect from the sample heater, we measured the thermal power and thermal conductivity with different heater currents (as shown in Fig. 3). The transition temperature T_s for thermal power is defined as the temperature when the entire sample enters the metallic states. Figure 3(a) shows T_s shifts towards lower temperature with higher heater power. A similar effect is also observed in thermal conductivity. The thermal conductivity peak position T_κ moves towards lower temperature and broadens with higher heater power. Because of the sample heater, the real temperature of the sample could be higher than the temperature reading from the thermometer on the probe. So, we plot the temperature difference between the two thermocouples ΔT_{th} vs. the heater power on the right axes of Figs. 3(c) (warm-up) and 3(d) (cool-down). During warm-up, when the heater power increases from 2 mW to 8 mW, ΔT_{th} increases by 3.5 K. The transition temperatures T_s and T_κ are plotted on the left axes of Figs. 3(c) (warm-up) and 3(d) (cool-down). T_s decreases about 4.5 K and T_κ decreases by 3.7 K when the heater power changes from 2 mW to 8 mW. So, the shift of T_s and T_κ is mainly due to the self-heating coming from the sample heater. The reason why the thermal conductivity peaks become broader with higher heater power is that the enhancement of thermal conductivity only happens in a very narrow temperature range, and the ac current in the sample heater changes the sample temperature during one period, which artificially broadens the peak. This heating effect also explains the difference of T_s values observed in the electrical resistivity and that of the Seebeck effect shown in Figs. 2(a) and 2(b).

To further understand the origin of the thermal conductivity peak, we measured the magnetic field dependence of the thermal conductivity up to 13.9 T with both longitudinal and transverse configurations. When H is parallel to the heat current I_Q, the peak position and width do not show obvious change with respect to the magnetic field [Fig. 4(a)]. With H perpendicular to I_Q, the thermal conductivity peak becomes slightly lower and shifts towards lower temperature [as shown in Fig. 4(b)]. In order to verify whether this change is due to the magnetic field or sample degradation,[21] we did the field dependent measurement with a sequence of magnetic field equal to 0 T, 5 T, 9 T, 13.9 T, and 0 T. We found that the peak height always becomes lower and the position keeps on shifting towards lower temperature. Thermal cycles could bring a considerable amount of thermal shock to the sample, which induces dislocation strain fields in it and decreases the thermal conductivity.[21] So, the lowering of the thermal conductivity peak in different thermal cycles should come from the sample degradation. The contribution to the thermal conductivity peak could come from neutral heat carriers since it does not respond to the magnetic field.

One significant feature of the enhancement of the thermal conductivity is that it only happens during the MIT, around where VO_2 undergoes a structural transition from the low-temperature rutile phase to the high-temperature tetragonal phase. The kinetic model relates the thermal conductivity κ to the heat capacity C as

$$\kappa \sim \frac{1}{3} C v l, \tag{1}$$

with v being the average velocity and l the mean free path. The sharp peak of κ at the MIT cannot be completely explained by the divergence of C at the first-order phase

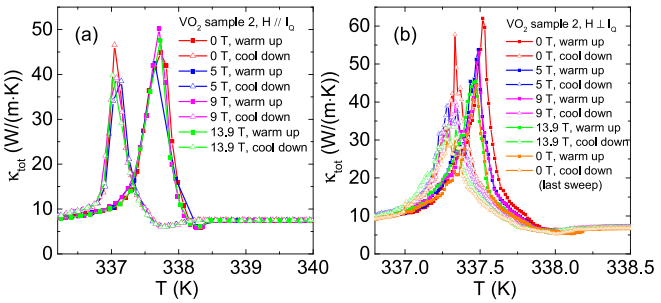

FIG. 4. Magnetic field dependence of the total thermal conductivity κ_{tot} vs. T in VO_2 sample 2 with H (a) parallel to the heat flow I_Q and (b) perpendicular to the heat flow I_Q.

transition because the heat capacity peak in VO_2 is much weaker than our 8–9 times enhancement peak in the thermal conductivity.[1,29] Similar enhancement of thermal conductivity at high temperature was also observed around the α-β phase transition in Cu_2Se and $Cu_{1.98}Ag_{0.2}Se$ between 350 K and 400 K,[22] while the origin of this peak was not quite discussed yet. But a significant reduction of the thermal conductivity is observed in PbTe[27] and $Pb_{1-x}Ge_xTe$[28] alloys, and this change was argued to arise from the fact that the softening of optical mode can increase anharmonic acoustic-optical coupling and decrease phonon lifetimes. On the theory side, Eq. (1) assumes a homogeneous and isotropic conduction media. The structural phase transition in VO_2 indicates an inhomogeneous media. The mean free path l is at best the same and could become much smaller during the transition.

The acoustic phonons already carried heat current in the insulating and metallic states. It is hard to figure out the mechanism that can reduce the scattering rate of acoustic phonons by a factor of 8–9 only at the MIT transition. Therefore, we hypothesize that the strong enhancement of κ in VO_2 can be explained by a large group velocity increase at the transition, which is likely a consequence of the softening optical phonon modes that were observed by neutron scattering[12] in VO_2. Generally, when the crystal structure undergoes a transition that is associated with softening of the optical phonons, the population n and velocity v of these phonon modes increase greatly. The phonon thermal conductivity is $\kappa_{ph} \propto \frac{1}{k_B T^2} \sum n(n+1)(\hbar\omega)^2 v l$, with $\hbar\omega$ being the phonon energy.[26] As a result, the increase in additional softened phonons, as well as the phonon velocity, would likely to contribute to the enhancement of the thermal conductivity. For example, silica involves from the low-pressure stishovite phase to the high-pressure $CaCl_2$-type phase under hydrostatic compression.[23–25] Recently, Aramberri *et al.* carried out first-principles calculations and reported that in silica, the longitudinal component of thermal conductivity κ increases about 2 orders of magnitude at the critical pressure P_c and $T = 10$ K.[26] At the structural transition point, because of the instability of the lattice, the softening of some acoustic modes is overcompensated by a large increase in their population, which strongly enhances the low-temperature thermal conductivity of silica. However, for VO_2, the phase transition happens at a much higher temperature, and other factors could dominate the contribution of thermal conductivity. Aramberri *et al.*[26] also point out that when three-phonon scattering dominates the scattering process, the mode softening can close the phonon-phonon scattering channels and increase the thermal conductivity. The increase in phonon population due to softening could bring a substantial enhancement in the heat capacity. Given such a high increase in heat capacity around MIT and non-zero group velocity, the softened phonons could carry a huge amount of heat which results in the peak in the thermal conductivity. One example is the thermal conductivity peak near the Peierls transition in two charge-density-wave systems $K_{0.3}MoO_3$ and $(TaSe_4)_2I$.[30] The author claimed that the anomalous peak is due to the increase in phonon mode population rather than changes in the electron- or phonon-scattering process. A first-principles calculation would help to fully understand the mechanism behind the enhancement of the thermal conductivity in VO_2.

All the electronic devices or circuitry could generate excess heat while operating, so the thermal management is essential to their reliability.[31] Our discovery provides a general idea of the realization of high thermal conductivity materials. Working at the structural transition point of phase change materials could potentially create a thermal path to efficiently conduct the heat outside the material and make the device work at an optimal temperature. The low-frequency phonons usually dominate the heat transport, so the soft modes in materials like VO_2 suggest potential applications in temperature-tunable thermal switches.[32]

We did the electrical and thermal transport measurements in VO_2 single crystals. The electrical conductivity is enhanced at the transition by a factor of 10^4–10^5, accompanied by a sharp drop of the thermal power S. By conducting the thermal transport measurement with an extremely slow sweeping speed of temperature, a narrow thermal conductivity peak is revealed within the MIT of VO_2 single crystals. The thermal conductivity was measured in a magnetic field up to 13.9 T parallel or perpendicular to the heat current, which did not show obvious dependence on H. This indicates that the strong enhancement of the thermal conductivity could possibly be due to the softening of certain phonon modes at the phase transition[26–28] and induce a strong enhancement of the thermal conductivity.

This work was mainly supported by the Office of Naval Research through the Young Investigator Prize under Award No. N00014-15-1-2382 (thermal transport and electrical transport measurements). The sample growth in UTK was supported by NSF-DMR-1350002 (sample growth). The measurement instrument benefits from the National Science Foundation Major Research Instrumentation Award under No. DMR-1428226 (supports the purchase of the PPMS). Q.H. acknowledges the support from the Go students program of ORNL.

[1]C. N. Berglund and H. J. Guggenheim, Phys. Rev. **185**, 1022 (1969).
[2]J. B. Goodenough, J. Solid State Chem. **3**, 490–500 (1971).
[3]S. Lee, K. Hippalgaonkar, F. Yang, J. Hong, C. Ko, J. Suh, K. Liu, K. Wang, J. J. Urban, X. Zhang, C. Dames, S. A. Hartnoll, O. Delaire, and J. Wu, Science **355**, 371–374 (2017).
[4]K. Shibuya, M. Kawasaki, and Y. Tokura, Appl. Phys. Lett. **96**, 022102 (2010).
[5]Y. Muraoka and Z. Hiroi, Appl. Phys. Lett. **80**, 583 (2002).
[6]M. Nakano, K. Shibuya, D. Okuyama, T. Hatano, S. Ono, M. Kawasaki, Y. Iwasa, and Y. Tokura, Nature **487**, 459–462 (2012).

[7]M. Nakano, K. Shibuya, N. Ogawa, T. Hatano, M. Kawasaki, Y. Iwasa, and Y. Tokura, Appl. Phys. Lett. **103**, 153503 (2013).
[8]T. Nan, M. Liu, W. Ren, Z.-G. Ye, and N. X. Sun, Sci. Rep. **4**, 5931 (2014).
[9]K. Kawatani, T. Kanki, and H. Tanaka, Phys. Rev. B **90**, 054203 (2014).
[10]V. R. Morrison, R. P. Chatelain, K. L. Tiwari, A. Hendaoui, A. Bruhács, M. Chaker, and B. J. Siwick, Science **346**, 445 (2014).
[11]C. J. Hearn, J. Phys. C: Solid State Phys. **5**, 1317 (1972).
[12]J. D. Budai, J. Hong, M. E. Manley, E. D. Specht, C. W. Li, J. Z. Tischler, D. L. Abernathy, A. H. Said, B. M. Leu, L. A. Boatner, R. J. McQueeney, and O. Delaire, Nature **515**, 535 (2014).
[13]Y. Bando, K. Nagasawa, Y. Kato, and T. Takada, Jpn. J. Appl. Phys. **8**, 633 (1969).
[14]K. Nagasawa, Mater. Res. Bull. **6**, 853 (1971).
[15]D. Zhao, X. Qian, X. Gu, S. A. Jajja, and R. Yang, J. Electron. Packag. **138**(4), 040802 (2016).
[16]C. Yin, R. Zhang, G. Qian, Q. Fu, C. Li, M. Wang, C. Zhu, L. Wang, S. Yuan, X. Zhao, and H. Tao, Appl. Phys. Lett. **110**, 172404 (2017).
[17]J. Cao, W. Fan, H. Zheng, and J. Wu, Nano Lett. **9**, 4001 (2009).
[18]T. Katase, K. Endo, and H. Ohta, Phys. Rev. B **92**, 035302 (2015).
[19]D. Fu, K. Liu, T. Tao, K. Lo, C. Cheng, B. Liu, R. Zhang, H. A. Bechtel, and J. Wu, J. Appl. Phys. **113**, 043707 (2013).
[20]V. N. Andreev, A. V. Chudnovskii, A. V. Petrov, and E. I. Terukov, Phys. Status Solidi A **48**, K153–K156 (1978).
[21]H. Jin, O. D. Restrepo, N. Antolin, S. R. Boona, W. Windl, R. C. Myers, and J. P. Heremans, Nat. Mater. **14**, 601–606 (2015).
[22]S. Ballikaya, H. Chi, J. R. Salvadorc, and C. Uher, J. Mater. Chem. A **1**, 12478 (2013).
[23]M. A. Carpenter, R. J. Hemley, and H.-K. Mao, J. Geophys. Res.: Solid Earth **105**, 10807, https://doi.org/10.1029/1999JB900419 (2000).
[24]D. Andrault, G. Fiquet, F. Guyot, and M. Hanfland, Science **282**, 720 (1998).
[25]A. Togo, F. Oba, and I. Tanaka, Phys. Rev. B **78**, 134106 (2008).
[26]H. Aramberri, R. Rurali, and J. íñiguez, Phys. Rev. B **96**, 195201 (2017).
[27]R. M. Murphy, E. D. Murray, S. Fahy, and I. Savić, Phys. Rev. B **93**, 104304 (2016).
[28]R. M. Murphy, E. D. Murray, S. Fahy, and I. Savić, Phys. Rev. B **95**, 144302 (2017).
[29]G. V. Chandrashekhar, H. L. C. Barros, and J. M. Honig, Mater. Res. Bull. **8**, 369 (1973).
[30]R. S. Kwok and S. E. Brown, Phys. Rev. Lett. **63**, 895 (1989).
[31]Y. A. Cengel and A. J. Ghajar, *Heat and Mass Transfer: Fundamentals and Applications*, 5th ed. (McGraw-Hill Education, 2014), Chap. 15.
[32]G. Venkataraman, Bull. Mater. Sci. **1**, 129 (1979).